International Orthopaedics (SICOT) (2013) 37:753–759
DOI 10.1007/s00264-012-1751-y

ORIGINAL PAPER

Prevascularisation with endothelial progenitor cells improved restoration of the architectural and functional properties of newly formed bone for bone reconstruction

Hao Pang · Xue-Hui Wu · Sheng-Long Fu · Fei Luo · Ze-Hua Zhang · Tian-Yong Hou · Zhi-Qiang Li · Zheng-Qi Chang · Bo Yu · Jian-Zhong Xu

Received: 16 October 2012 / Accepted: 5 December 2012 / Published online: 4 January 2013

Abstract
Purpose The aim of this study was to examine whether the addition of endothelial progenitor cells (EPCs) contributes to restoring the architectural and functional properties of newly formed bone for reconstruction of bone defects.
Methods Bone marrow-derived EPCs and mesenchymal stem cells (MSCs) were co-seeded onto demineralized bone matrix (DBM) as a prevascularized tissue-engineered bone (TEB) for the repair of segmental bone defects to evaluate the effects of prevascularization of TEB on ameliorating morphological, haemodynamic and mechanical characteristics.
Results The restoration of the intraosseous vasculature and medullary cavity was improved markedly compared to the non-prevascularized groups. The blood supply, biomechanical strength, and bone mineral density of the prevascularized group were significantly higher than those of the non-prevascularized groups during bone reconstruction.
Conclusions The present study indicates that EPC-dependent prevascularization contributes to bone healing with structural reconstruction and functional recovery and may improve the understanding of correlation between angiogenesis and osteogenesis.

Electronic supplementary material The online version of this article (doi:10.1007/s00264-012-1751-y) contains supplementary material, which is available to authorized users.

Hao Pang and Xue-Hui Wu contributed equally to this work.

H. Pang · X.-H. Wu · S.-L. Fu · F. Luo · Z.-H. Zhang · T.-Y. Hou · Z.-Q. Li · Z.-Q. Chang · B. Yu · J.-Z. Xu (✉)
Department of Orthopaedics, Southwest Hospital,
The Third Military Medical University, Chongqing, China
e-mail: xujianzhong1962@163.com

Introduction

Despite intense research efforts, the repair of large bone defects is still not satisfactory and remains a major orthopaedic challenge [1]. Tissue-engineered bone has emerged as an effective strategy to overcome the challenge, but the vascularization of bone graft is an obstacle which restricts its performance [2]. One possible way to address this issue is the use of endothelial progenitor cells (EPCs), which have the ability to form endothelial colonies in vitro and contribute to revascularization in vivo [3].

A number of investigators have shown that EPCs enhanced bone formation to bridge bone defects for bone repair [4, 5]. However, most current studies have highlighted the importance of improving bone formation, while few studies have further examined the structure and function of newly formed bone tissue. The natural process of skeletal repair suggests that bone formation does not mark the completion of bone repair. Truly successful reconstruction of bone defects can only be signified by the re-establishment of normal tissue structures, including intraosseous vasculature and medullary cavity. Although EPCs have been increasingly used for organ vascularization and regeneration since they were first described and characterized by Asahara et al. in 1997 [6, 7], the effect of EPCs on regaining intraosseous vessels and blood supply is still unknown. Also unknown is whether the addition of EPCs could be helpful for restoration of the medullary cavity and biomechanical properties during bone healing.

In this study, we prepared prevascularized scaffolds with EPCs and determined if they could facilitate the restoration of the intraosseous vasculature and blood supply during reconstruction of critical-sized bone defects. Furthermore,

we preliminarily observed the effect of EPCs on the biomechanical strength and bone mineral density (BMD). Our findings indicated that EPC-dependent prevascularization has greatly enhanced the recovery of intraosseous circulation and the medullary cavity with increasing the biomechanical strength and BMD during bone healing.

Materials and methods

Preparation of demineralized bone matrix (DBM) scaffolds

A DBM scaffold was prepared through demineralization of cancellous bone from a mature healthy rabbit and the demineralized procedure was carried out with strict asepsis, as previously described [8]. The prepared DBM was cut up into blocks with a size of 15 mm×5 mm×5 mm for construction of tissue-engineered bone (TEB). The microstructures of the DBM were visualized under a scanning electron microscope (SEM) (KYKY-EM3200, KYKY Technology Development Ltd., Beijing, China).

Cell preparation and characterization

Bone marrow was aspirated sterilely from iliac crests of healthy New Zealand white rabbits and subjected to density gradient centrifugation in Percoll (density=1.077 g/mL; Sigma, USA) at 400 g for 20 minutes at room temperature. Then, the mononuclear cells (MNC) were isolated from the buffy coat between the Percoll solution and the blood plasma and washed thrice with PBS, and cultured in a humidified 37 °C, 5 % CO_2 incubator with 0.25 % trypsin plus 0.01 % EDTA for subculture until cells reached about 80–90 % confluence.

EPCs were obtained by culturing bone marrow MNC in endothelial cell growth medium-2 (EGM-2, Cambrex, USA) with SingleQuots growth supplements (Cambrex, USA) on fibronectin-coated plates. After six days culture, EPCs were identified by immunohistochemical staining for VEGFR-2 (vascular endothelial growth factor receptor 2) (Abcam, CA, UK) and vWF (von Willebrand Factor) (Santa Cruz, USA). The uptake of Dil-ac-LDL (Dil-labeled acetylated low-density lipoprotein) (Molecular Probes, USA) and FITC-UEA-1 (FITC-labeled Ulex Europaeus Agglutinin 1) (Vector, USA) was also used for EPC identification.

In order to obtain mesenchymal stem cells (MSCs), bone marrow-derived MNCs were cultured in Dulbecco's modified Eagle's medium/Ham's F-12 nutrient mixture (1:1; DMEM/F-12) (Hyclone, USA), supplemented with 10 % fetal bovine serum (FBS), 0.1 μM dexamethasone, 10 mM Beta-glycerophosphate, and 50 μM ascorbic acid. The osteogenic differentiation ability of MSCs was characterized by immunohistochemistry for osteocalcin (a protein made exclusively by MSCs/osteoblasts) (Abcam, UK) and identification of calcium nodus with alizarin red S staining and the tetracycline fluorescence labeling.

Construction of implants

The bone marrow-derived EPCs and MSCs were respectively resuspended at the concentration of 5×10^6 cells/mL for constructing TEB. Three construct types were prepared: (1) 100 μL EPCs + 100 μL MSCs + DBM, (2) 200 μL MSCs + DBM, and (3) DBM without cells. The tissue-engineered bones were incubated at 37 °C in 5 % CO_2 for four hours to allow for cell adherence.

Animals and operative procedures

This study was carried out in strict accordance with the recommendations in the Guide for the Care and Use of Laboratory Animals of the National Institutes of Health. In the protocol, all efforts were made to ameliorate animal suffering. Diaphyseal defects (15 mm long) were created on the bilateral radii of 24 healthy New Zealand white rabbits under aseptic conditions after the rabbits were anaesthetized intravenously with 3 % sodium pentobarbital (1 mL/kg).

On the basis of a pair-matched crossover design, 48 radial diaphyseal defects were randomized into three groups as follows. In group A, prevascularized TEB (EPCs+MSCs+DBM) was implanted into the bone defects (n=16). In group B, non-prevascularized TEB (MSCs+DBM) was implanted (n=16). In group C, DBM without cells was implanted for control (n=16). The 15-mm defect was considered to be critical and cannot be reconstructed spontaneously in the absence of bone-repair materials [9]; thus, no control group without bone grafts was constituted in this study on the basis of ethical consideration.

Radiographic analysis

The rabbits were radiographed in the prone position at two to 12 weeks postoperatively to observe the osteogenesis and recanalization of the medullary cavity. Each radiograph was examined by two independent observers who were blind to treatment type and given a score based on a radiographic scoring system (Lane and Sandhu) [10] (detailed in Table 1).

Chinese ink microangiography

After the bilateral axillary arteries were exposed and inserted with a 1.0 mm catheter, a mixture of Chinese ink and distilled water (7:3, v/v) was injected into the axillary artery, by the modified methods according to the reference [11, 12]. Upon completion of perfusion, the radii were fixed with 10 % formalin solution for one week, decalcified with 5 % hydrochloric acid for five days, dehydrated in gradient

Table 1 Radiographic scoring system

Parameter	Classification	Score
Bone formation	None	0
	25 % of defect	1
	50 % of defect	2
	75 % of defect	3
	Full	4
Persistence of the fracture line	Full fracture line	0
	Partial fracture line	2
	Absent fracture line	4
Bone remodeling	None	0
	Intramedullary canal	2
	Full cortex	4

alcohol for two days, vitrified by dimethylbenzene for one day, deposited in holly oil, and cut to yield 100μm thick cross-sections for observation.

Immunohistochemistry analysis

Specimens from the bone defect sites were fixed with 10 % formalin for one week, decalcified with 5 % nitric acid for five days, dehydrated with gradient ethanol solutions for two days, embedded in paraffin, and cut to yield 2-μm thick sections. For immunohistochemical analysis, the sections were treated with mouse anti-rabbit primary IgG for vascular endothelial growth factor (VEGF) and Factor VIII (FVIII) (Santa Cruz, USA) and observed under light microscope.

Radionuclide bone imaging

The radionuclide bone imaging was carried out by a Millennium/MPR SPECT (GE, Piscataway, NJ) and analysed with the eNTEGRA work-station after injection of 1 mCi/kg technetium-99m methylene diphosphonate (^{99m}Tc-MDP, Beijing Atom-Hitech Company, Beijing, China) into the ear vein, as we have described previously [8]. One frame per minute blood pool images for two minutes, followed by metabolic phase images (one frame per five minutes) at three hours were recorded. Later, a region of interest (ROI) of the reconstructed radius and the ipsilateral healthy hip was drawn on the blood-pool and metabolic phase images. The count uptake ratio was defined as ROI of the reconstructed radius divided by the ipsilateral healthy hip, and the mean ratio from three images was used for comparison.

Biomechanical and BMD evaluation

Torsional mechanical testing was performed using a testing machine RG 1-5A (Reger, Shenzhen, China) at 12 weeks after the surgery (four samples for each groups), according to our previously described procedure [8]. Torque was measured by rotating the long axis of the bone at an angular velocity (1°/s) until failure. The maximum torsional strength of radii from all three groups was recorded in a computerized data collection system for comparison. The bone mineral densities (BMD) of the newly formed bone in the defect were measured at two, four, eight and 12 weeks postoperatively with the dual energy X-ray absorptiometry (LEXXOS, DMS, France).

Statistical analysis

All data are reported as mean±standard deviation (SD). The data of multiple comparisons were analysed using ANOVA and Dunnett's post hoc test. Mann–Whitney *U*-test for ordinal scaled measurements was used to assess statistical significance for the radiographic scoring at different time points. All tests were performed by SPSS and the level of significance was defined at $p<0.05$.

Results

DBM preparation

DBM was prepared through demineralization of rabbit cancellous bone with a size of 15 mm×5 mm×5 mm (Fig. 1a). SEM analysis showed that the average pore size of DBM scaffold was in the range of 300–800 μm with 70 % porosity (Fig. 1b). DBM typically is of low radiographic density on the radiograph (Fig. 1d), which is convenient to better observe the natural process of osteogenesis and recanalization of the medullary cavity.

Cell isolation and characterization

The bone marrow-derived EPCs tended to grow in clusters at three days (Fig. 2a), expressed the typical EPC phenotypic markers, VEGFR-2 (Fig. 2b) and vWF (Fig. 2c) at six days, and were double-positive to both FITC-UEA −1 (Fig. 2d) and Dil-ac-LDL (Fig. 2e).

After five-day culture, MSCs exhibit a spindle-shaped appearance (Fig. 2g) with the capacity of osteogenic differentiation, which was assessed by osteocalcin immunohistochemistry (Fig. 2h). The calcified nodules formed under the conditional culture were characterized by alizarin red S staining (Fig. 2i) and tetracycline fluorescence staining (Fig. 2j).

Radiographic examination

Radiographic analyses were used to evaluate the osteogenesis and recanalization of the medullary cavity (Fig. 3). Although the area of bone defects were successfully bridged with continuous bony callus in all three groups at week eight, only the

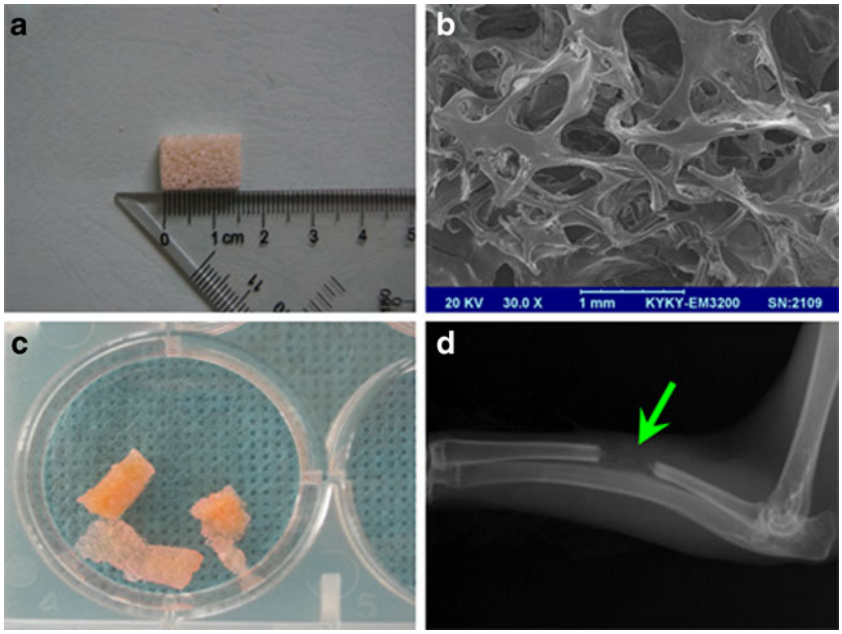

Fig. 1 Demineralized bone matrix (DBM) preparation and characterization. **a** DBM was prepared with a size of 15 mm× 5 mm×5 mm. **b** SEM analysis showed that DBM had 70 % porosity with 300–800 μm pore size; bar length = 1 mm. **c** Macromorphology of DBM seeded with cells. **d** DBM displayed low radiographic density on the radiograph (at two weeks after operation)

medullary cavity in group A was partly recanalized. At week 12, the medullary cavity in group A was completely recanalized, the medullary cavity in group B was partly (<50 %) recanalized and group C was nearly not recanalized. The radiographic scores increased with time in each group, with group A>group B>group C ($P<0.05$) at each time point.

Microangiographic evaluation

Representative axial views of Chinese-ink microangiographs at 12 weeks showed that the cross-sectional morphology of the medullary cavity and intraosseous vasculatures, including intramedullary blood vessels, in group A (Fig. 4b) was renewed close to normal (Fig. 4a). However, the medullary vessels and medullary cavity were partly restored in group B (Fig. 4c) and barely rebuilt in group C (Fig. 4d).

Immunohistochemistry observation

The areas of early vascularization in each group were immunohistologically evaluated by VEGF and FVIII. At two

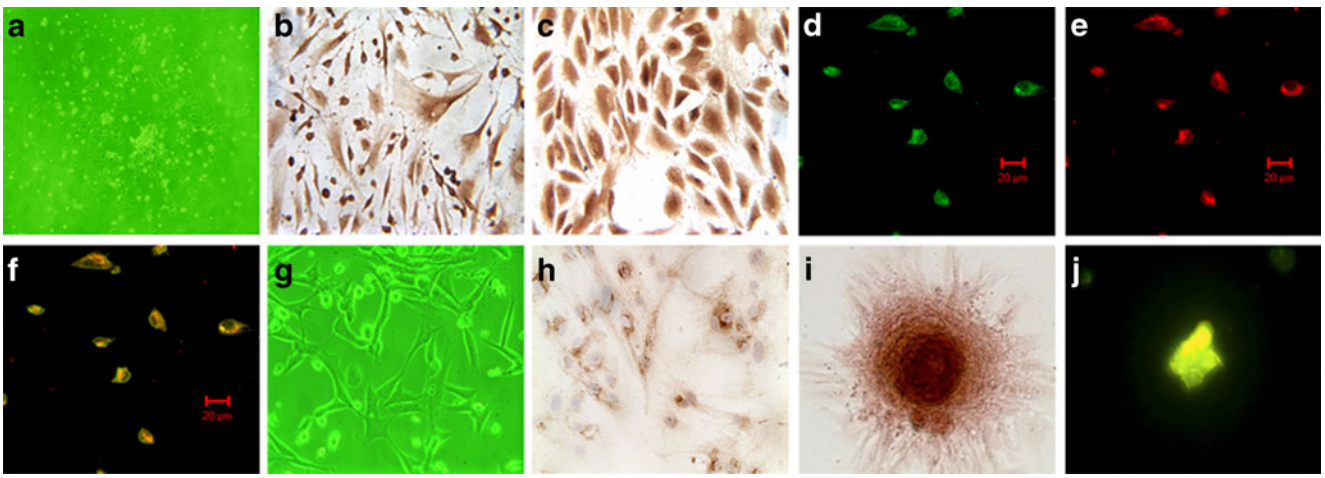

Fig. 2 Cell culture and characterization. The first passage endothelial progenitor cells (EPCs) began to grow clusters after three day culture (**a**, 100×) and stain positive for VEGFR-2 (**b**, 400×) and vWF(**c**, 400×) at six days. The FITC-UEA-1/Dil-ac-LDL double-positive fluorescence staining displayed EPCs. FITC-UEA-1 show green fluorescence (**d**); Dil-ac-LDL display red fluorescence (**e**); EPCs were dual positive and exhibited orange fluorescence (**f**); bar length = 20 μm. **g** The appearance of MSCs (100×) at five days. The osteogenic differentiation ability of MSCs was verified immunohistochemically by osteocalcin staining (**h**). The MSCs formed calcium nodes and were characterized by alizarin red S staining and the tetracycline fluorescence labeling. A pink calcium nodus appears by alizarin red S staining (**i**), and a brilliant yellow calium nodus appears by tetracycline fluorescence staining (**j**)

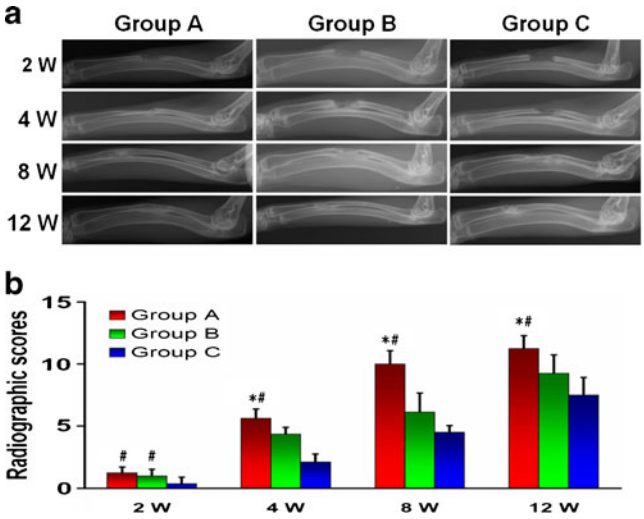

Fig. 3 Radiographic analysis. The changes of the defect areas and medullary cavity of rabbit radius at two to 12 weeks postoperatively were detected by X-ray radiographs (**a**). There was no evident difference between groups A and B at two weeks after operation, but radiographic scores in group C are obviously less than those of the two groups. After week four, the radiographic scores in group A have scored significantly higher than both B and C groups (**b**). *$P<0.05$ compared to group B, #$P<0.05$ vs. group C

weeks, early vascularization was enhanced by prevascularized TEB, with a neovascularization that expressed higher VEGF (Fig. 4e) and FVIII (Fig. 4h) immunopositivity in comparison with non-prevascularized tissue in group B (Fig. 4f, i) and C (Fig. 4g, j).

Radionuclide bone imaging

Blood pool imaging and metabolic phase imaging were conducted to evaluate the blood supply of bone tissue and bone viability at two to eight weeks after operation. For blood pool imaging, the count uptake ratio of ROI in group A was significantly higher than that in group B and C at weeks two, four and eight postoperatively ($P<0.05$) (Fig. 5a). For metabolic phase imaging, similarly, the count uptake ratio of ROI in group A markedly exceeded that in group B and C at 2–8 postoperative weeks ($P<0.05$) (Fig. 5b).

Biomechanical and BMD assessment

Torsional mechanical testing was conducted on each harvested sample. The EPC treatment group had a significantly higher torsional strength when compared with groups B ($P=0.023$) and C ($P=0.000$) (Fig. 5c). Bone mineral density (BMD) of the defect site also revealed significant differences between groups A and other experimental groups. At two postoperative weeks, the BMD of groups A and B was significantly higher than that of group C, subsequently, the BMD of group A was significantly higher than that of groups B and C at four to 12 weeks ($P<0.05$) (Fig. 5d).

Discussion

Bone healing is a unique regenerative process which requires coordinated coupling between osteogenesis and

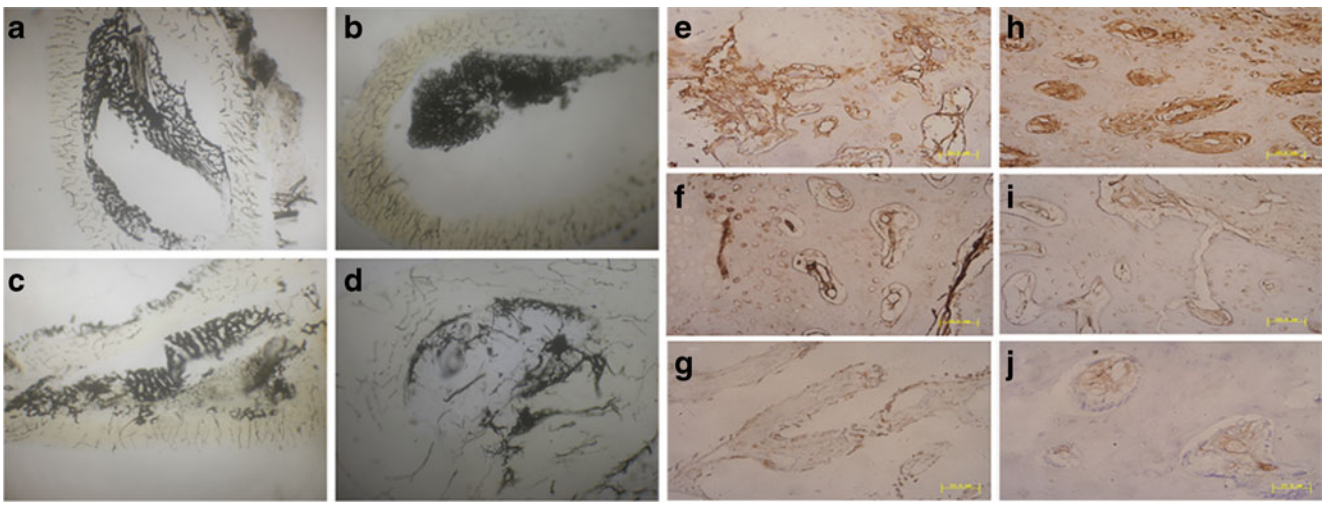

Fig. 4 Morphological and histological observation. Axial view (4× magnification) of Chinese-ink microangiographs at 12 weeks post operation showed that the cross-sectional morphology of the medullary cavity and intraosseous vasculatures, including intramedullary blood vessels in group A (**b**) was restored close to normal (**a**). However, the medullary vessels and medullary cavity were partly restored in group B (**c**) and barely rebuilt in group C (**d**). Early vascularization was enhanced by EPC prevascularization with formation of neovasculature expressed higher VEGF (**e**) and FVIII (**h**) immunopositivity at two weeks. In group B, the number of neovasculature was less than group A, and the expression of VEGF (**f**) and FVIII (**i**) was moderate positive. Few blood vessels with weakly positive expression of VEGF (**g**) and FVIII (**j**) could be observed in group C; bar length = 50 μm

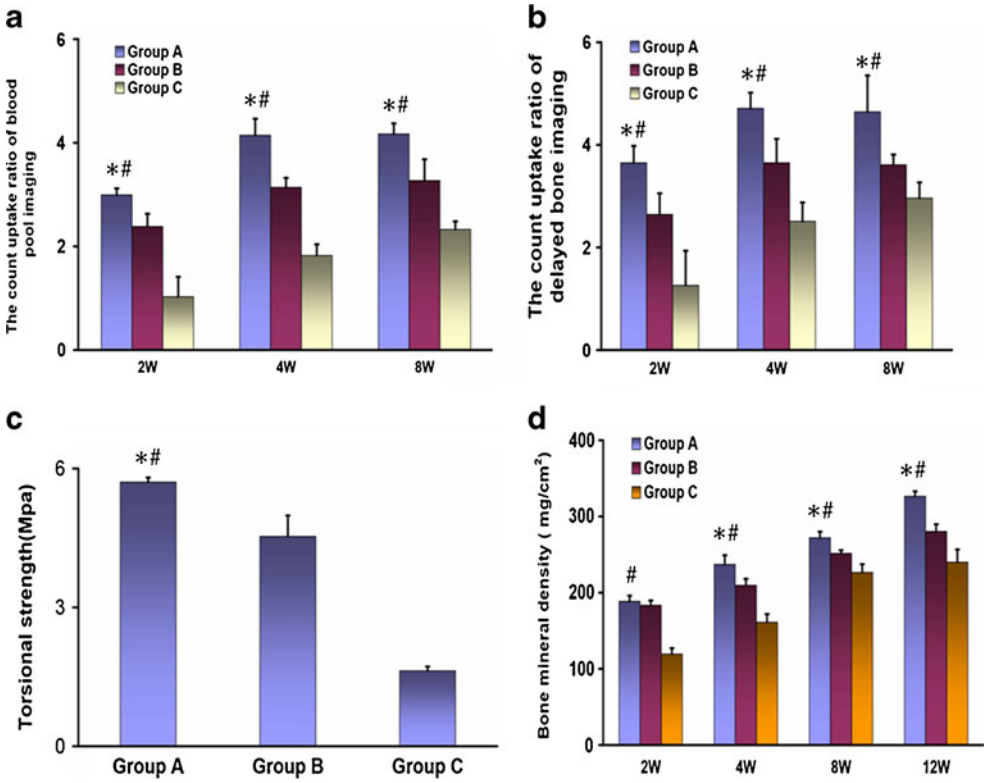

Fig. 5 Radionuclide bone imaging, biomechanical, and BMD evaluation. For blood pool imaging (**a**) and metabolic phase imaging (**b**), the count uptake ratio of ROI in group A was significantly higher than that in groups B and C at weeks two, four and eight postoperatively ($P<0.05$). The EPC treatment group also had a significantly higher torsional strength when compared with groups B ($P=0.023$) and C ($P=0.000$) (**c**). During four to 12 weeks postoperatively, BMD of rabbit radii in group A were significantly higher than that of groups B and C (**d**). *$P<0.05$ compared to group B, #$P<0.05$ vs. group C

angiogenesis [5, 13]. Angiogenesis, a physiological process involving the formation of neovasculature from existing vasculature, precedes bone formation and leads bone regeneration to improve bone defect healing [14–16]. EPCs are identified as a population of pluripotent progenitors that are capable of inducing in vivo angiogenesis, so prevascularizing TEB with EPCs is a promising strategy to accelerate angiogenesis and osteogenesis. In the present report, we prevascularized MSCs-based TEB with bone marrow-derived EPCs and examined the effect of prevascularization on structure and function recovery of newly formed bone. The results clearly indicated that the addition of EPCs contributed to enhance reestablishment of intraosseous circulation and medullary cavity of bone tissue as well as increased the biomechanical strength and BMD during bone reconstruction.

The transplantation of EPCs has been shown to improve circulation status and blood supply of the ischemic tissue [7]. However, there were few reports about the effect of EPCs delivery on intraosseous angiogenesis and blood supply in the newly formed bone. For bone repair, achieving the vascularization of tissue-engineered bone is not only a matter of meeting the nutritional requirements of tissues, but also a matter of realizing structure, form and function reconstruction [17]. In the present study, radiographic analysis showed that the presence of EPCs resulted in an earlier recanalization of medullary cavity. In accordance with the results, the results of Chinese-ink microangiography further demonstrated that medullary cavity and intraosseously vascular system, even the intramedullary vasculatures, in the EPC-prevascularized group was rebuilt earlier than other groups. We also observed a significant increase of capillary vessels with VEGF and FVIII immunopositivity in comparison with non-prevascularized tissue at an early stage after implantation.

The effect of EPCs prevascularization on blood supply was assessed by radionuclide bone scanning to observe the degree of achieved vascular improvement. The results of blood pool images, which represent the status of blood supply, demonstrated that the addition of EPCs significantly increased the blood supply to the bone defect during bone regeneration. The results of metabolic phase images, which index the outcome of osteogenesis, verified that osteogenesis of the defect site in the EPC-prevascularized group was superior to that of the non-prevascularized group.

The restoration of bone biomechanical properties may also serve as a sign for successful bone regeneration [18]. In our study, we observed that prevascularized TEB had exceedingly positive effects on restoration of biomechanical strength of new bone. We also identified an increase of BMD over the 12-week postoperative period, which may indirectly reflect the changes of the bone strength during fracture healing. The BMD of prevascularized samples was also greatly enhanced compared to other groups.

Our findings indicate that prevascularization with EPCs promotes the reconstruction of rabbit critical-sized radius

defects with successful restoration of intraosseous circulation and medullary cavity of bone tissue as well as increases the biomechanical strength and BMD. The results suggest that the prevascularized TEB with EPCs was superior to two other non-prevascularized implants for bone reconstruction.

Acknowledgments This study was financially supported by the National Natural Science Foundation of China (No. 81071465).

References

1. Pang H, Wu XH, Xu JZ (2012) A strategy for promoting bone regeneration by inducible expression of 15-LOX-1. Med Hypotheses 79(3):413–414
2. Santos MI, Reis RL (2010) Vascularization in bone tissue engineering: physiology, current strategies, major hurdles and future challenges. Macromol Biosci 10(1):12–27
3. Goon PK, Lip GY, Boos CJ, Stonelake PS, Blann AD (2006) Circulating endothelial cells, endothelial progenitor cells, and endothelial microparticles in cancer. Neoplasia 8(2):79–88
4. Rozen N, Bick T, Bajayo A, Shamian B, Schrift-Tzadok M, Gabet Y, Yayon A, Bab I, Soudry M, Lewinson D (2009) Transplanted blood-derived endothelial progenitor cells (EPC) enhance bridging of sheep tibia critical size defects. Bone 45(5):918–924
5. Atesok K, Li R, Stewart DJ, Schemitsch EH (2010) Endothelial progenitor cells promote fracture healing in a segmental bone defect model. J Orthop Res 28(8):1007–1014
6. Asahara T, Murohara T, Sullivan A, Silver M, van der Zee R, Li T, Witzenbichler B, Schatteman G, Isner JM (1997) Isolation of putative progenitor endothelial cells for angiogenesis. Science 275(5302):964–967
7. Rafii S, Lyden D (2003) Therapeutic stem and progenitor cell transplantation for organ vascularization and regeneration. Nat Med 9 (6):702–712
8. Hou T, Li Q, Luo F, Xu J, Xie Z, Wu X, Zhu C (2010) Controlled dynamization to enhance reconstruction capacity of tissue-engineered bone in healing critically sized bone defects: an in vivo study in goats. Tissue Eng A 16(1):201–212
9. Tu J, Wang H, Li H, Dai K, Wang J, Zhang X (2009) The in vivo bone formation by mesenchymal stem cells in zein scaffolds. Biomaterials 30(26):4369–4376
10. Lane JM, Sandhu HS (1987) Current approaches to experimental bone grafting. Orthop Clin N Am 18(2):213–225
11. Pazzaglia UE, Bonaspetti G, Ranchetti F, Bettinsoli P (2008) A model of the intracortical vascular system of long bones and of its organization: an experimental study in rabbit femur and tibia. J Anat 213(2):183–193
12. Pazzaglia UE, Congiu T, Marchese M, Zarattini G (2011) Structural pattern and functional correlations of the long bone diaphyses intracortical vascular system: investigation carried out with China ink perfusion and multiplanar analysis in the rabbit femur. Microvasc Res 82(1):58–65
13. Geris L, Gerisch A, Sloten JV, Weiner R, Oosterwyck HV (2008) Angiogenesis in bone fracture healing: a bioregulatory model. J Theor Biol 251(1):137–158
14. Kanczler JM, Oreffo RO (2008) Osteogenesis and angiogenesis: the potential for engineering bone. Eur Cell Mater 15: 100–114
15. Fayaz HC, Giannoudis PV, Vrahas MS, Smith RM, Moran C, Pape HC, Krettek C, Jupiter JB (2011) The role of stem cells in fracture healing and nonunion. Int Orthop 35(11): 1587–1597
16. Seebach C, Henrich D, Kahling C, Wilhelm K, Tami AE, Alini M, Marzi I (2010) Endothelial progenitor cells and mesenchymal stem cells seeded onto beta-TCP granules enhance early vascularization and bone healing in a critical-sized bone defect in rats. Tissue Eng A 16(6):1961–1970
17. Das A, Botchwey E (2011) Evaluation of angiogenesis and osteogenesis. Tissue Eng B Rev 17(6):403–414
18. Mavcic B, Antolic V (2012) Optimal mechanical environment of the healing bone fracture/osteotomy. Int Orthop 36(4): 689–695